OPEN

Metamaterials for Remote Generation of Spatially Controllable Two Dimensional Array of Microplasma

Pramod K. Singh[1], Jeffrey Hopwood[2] & Sameer Sonkusale[1]

[1]Nanolab, Department of Electrical and Computer Engineering, Tufts University, Medford, MA, USA-02155, [2]Plasma Engineering Laboratory, Department of Electrical and Computer Engineering, Tufts University, Medford, MA, USA-02155.

Since the initial demonstration of negative refraction and cloaking using metamaterials, there has been enormous interest and progress in making practical devices based on metamaterials such as electrically small antennas, absorbers, modulators, detectors etc that span over a wide range of electromagnetic spectrum covering microwave, terahertz, infrared (IR) and optical wavelengths. We present metamaterial as an active substrate where each unit cell serves as an element for generation of plasma, the fourth state of matter. Sub-wavelength localization of incident electromagnetic wave energy, one of the most interesting properties of metamaterials is employed here for generating high electric field to ignite and sustain microscale plasmas. Frequency selective nature of the metamaterial unit cells make it possible to generate spatially localized microplasma in a large array using multiple resonators. A dual resonator topology is shown for the demonstration. Since microwave energy couples to the metamaterial through free space, the proposed approach is naturally wireless. Such spatially controllable microplasma arrays provide a fundamentally new material system for future investigations in novel applications, e.g. nonlinear metamaterials.

Electromagnetic metamaterials are artificial composites made of sub-wavelength metallic structures in a host dielectric medium, engineered to achieve unusual properties not found in the nature. Initial efforts on metamaterial research were focused on the demonstration of negative refractive index[1–5] and building a perfect lens[2,5] or cloaking[3,6,7] device. However recently, metamaterials are also being widely studied for various practical applications such as perfect electromagnetic wave absorbers across the broad electromagnetic spectrum from microwave to optical wavelengths[8–11], modulators at terahertz frequencies[12,13], detectors and imagers[14–16], smart antennas and beam shaping devices[17,18]. Recently, O. Sakai et al. have employed metamaterial to realize negative permeability in the plasma medium to enhance microwave propagation and generation of high density plasma[19,20].

In this paper, we utilize metamaterials not as a medium but as a device, where it serves as an active substrate for the generation of plasma within each unit cell of the metamaterial. Metamaterials are typically employed to shape the electromagnetic fields as in the case with many of their prior applications[1–13]. However in this paper, we exploit one of the most interesting properties of metamaterials that of subwavelength localization of incident electromagnetic energy within the capacitive gap of each metamaterial unit cell at its resonance frequency as the source of energy to ignite and sustain microplasmas. This energy concentration can create sufficiently high electric field to ignite and sustain spatially confined non-thermal microplasmas within each unit cell of the metamaterial array structure. This energy localization at each unit cell of the metamaterial had been utilized in the past for realization of detectors and imagers[14–16].

Microplasma is loosely defined as plasma discharges with at least one characteristic dimension smaller than 1 mm and the goal is to be able to generate dense, stable plasmas at atmospheric or near-atmospheric pressures. The plasma medium consists of electrons, ions, molecules which interact strongly in the presence of electric and magnetic fields. For example, the excited electrons in the plasma medium emit light when they relax to the lower energy level and this light emission is an indication of presence of the plasma medium. Microplasma has been studied and used for a wide range of applications such as for material processing[21,22], plasma displays[21,23], medical treatment[24–30], ozone generation[31] for water treatment[32] and pollution control[21,33]. Recently, microplasmas have also been suggested for a new class of electronic transistors and devices[34–36]. Arrays of such microplasmas have significant benefits since they allow creation of plasmas over a large area for these applications. Currently, such
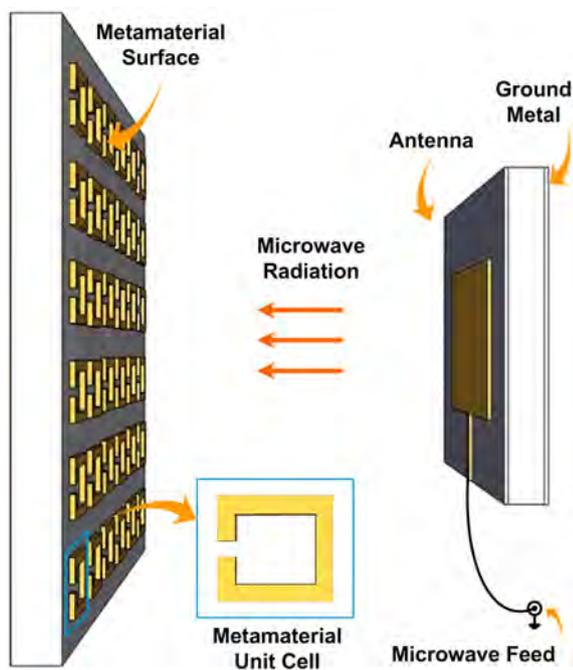
Figure 1 | Schematic representation of remote generation of plasma using metamaterials. Radiated microwave power from the antenna couples to the metamaterial at its resonance frequency and generates a high electric field inside the capacitive gap of each metamaterial unit cell (*i.e.*, C shaped split ring resonator). This ignites and sustains plasma that is localized in the sub-wavelength capacitive region of each metamaterial unit cell.

arrays have been demonstrated using dielectric barrier discharges (DBD), DC cavity microdischarges and microwave-frequency resonators. Among them, plasma generation using microwave-frequency resonators is highly promising since it allows plasma generation at low voltages in a wide range of environments[37,38] including air at atmospheric and near-atmospheric pressures. Microwave discharges provide long operational lifetime since the electrodes are not subjected to unwanted sputtering associated with other methods of plasma generation; this feature is attributed to the relative immobility of heavy ions in microwave fields. Stable arrays in both one and two dimensions have been demonstrated using a single input port for power and utilizing the inherent energy coupling between resonators - as governed by the principles of coupled mode theory - to share this power among the microplasmas in the array[39–41]. Spatial control of microplasmas in the one dimensional array has also been demonstrated through the embedding of solid state pin diodes for on/off control of individual resonators[34].

Metamaterials provide a simple realization of a large scale two dimensional array of microplasmas. In metamaterials, subwavelength resonators serve as meta-atoms of an artificial material with unique electromagnetic properties. In its most simplistic realization where the metamaterial is implemented as a single layer as a metasurface, the device is essentially a two dimensional array of resonators as shown in Fig. 1. When designed as an absorber at resonance, a metamaterial will absorb all the incident electromagnetic energy efficiently without reflection[8]. At resonance, the energy is concentrated in the subwavelength capacitive gap of each of the metamaterial unit cells. We explore this subwavelength localization of high microwave energy density to trigger and sustain microwave-frequency microplasmas. Since the incident electromagnetic energy couples through free space, an added significance of the work is wireless operation for the generation of an array of microplasmas on metamaterial substrate. An overall sketch for the free space excitation and remote generation of microplasmas in metamaterial is

shown in Fig. 1. The detailed experimental setup is shown in the supplementary section (Fig. S4).

Results

As shown in Fig. 1 the microwave energy is provided wirelessly from a patch antenna radiating in free space towards the metamaterial surface (or metasurface) which consists of a periodic distribution of unit cells made of 'C' shaped split ring resonators (SRR). Microwave energy coupled to the metamaterial generates a high electric field in the micrometer sized (150 microns) split gap of the SRR at the resonance frequency. When this electric field is high enough the argon gas atoms are ionized to form plasma in and around the gap region. Since metamaterials are inherently frequency selective, i.e. the energy coupling to it is maximum only at the resonance frequency of the individual resonators (or meta-atoms), one can engineer the metasurface to have more than one resonance frequency by using multiple resonators (or meta-atoms) in its realization where different meta-atoms are resonant at different frequencies. Moreover, one can also geometrically arrange these meta-atoms in a certain spatial pattern on this meta-surface for additional control over the geometrical pattern of microplasma. To verify the frequency selectivity, a dual frequency metamaterial is designed which contains two resonators that have distinct resonance frequencies (2.1 GHz and 2.45 GHz). When this metamaterial is irradiated by microwave energy, the plasma is generated in only the one set of resonators that has the same frequency as the incident microwave radiation. And when irradiated with microwave energy with a frequency of the second set of resonators, then the microplasmas are generated in the other set of resonators. Thus, one can spatially control the generation of microplasmas by choosing an appropriate frequency of incident radiation and placement of resonators in metamaterial array.

The photograph of the dual frequency metamaterial board is shown in Fig. 2 (a). Two resonators which are different in size result in two separate resonance frequencies. The larger size resonator has a lower resonance frequency (2.1 GHz). These two resonators are periodically distributed in a 2-dimensional array (any other pattern could also be chosen). The board consists of a 6 × 6 array of 36 resonators, 18 each for the two different resonance frequencies. For each C-shaped resonator, the width of metal line is tapered down to 0.7 mm from the original width of 1 mm near the capacitive gap to increase the energy concentration for microplasma generation. Two patch antennas are used to radiate microwave energy at two different resonant frequencies of the metamaterial that are used interchangeably. Simulation and measurement of the power transmission through the dual frequency metamaterial surface is shown in Fig. 2(b). It clearly shows two resonances, one at 2.1 GHz and another at 2.45 GHz. Small shifts in measured resonant frequency (0.01 GHz) are observed compared to simulation results due to process variations in the actual fabrication of the device. Electric field distribution is simulated at these two resonance frequencies (see supplementary section Fig. S1c). It shows that the electric field is significantly enhanced in the gap of the metamaterial resonators. The higher electric field is developed in the resonator only at its resonance frequency. At 2.1 GHz, higher electric field strength is developed in the gap of the larger resonator, and at 2.45 GHz it is developed in the gap of the smaller resonator (supplementary section Fig. S1c). There is also a finite but lower electric field generated in the gap of the resonators when excited at the resonance frequency of the other resonator. This undesired electric field is not sufficient to ignite the microplasma.

To radiate microwave power, two patch antennas are designed to wirelessly feed power to the metamaterial at two different resonance frequencies, 2.1 GHz and 2.45 GHz. (supplementary Fig. S2 and S3). Layout of the patch antenna is selected to provide wider bandwidth for wireless radiation.
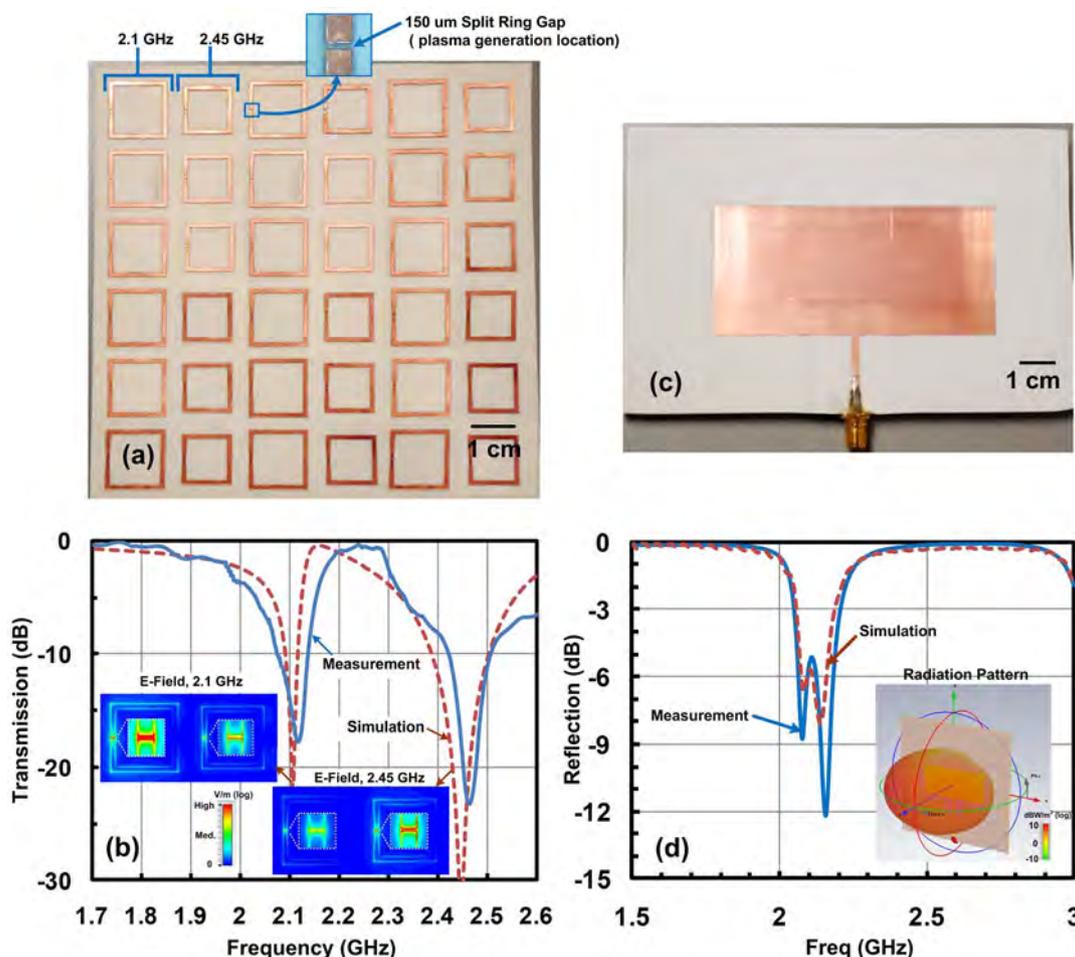
Figure 2 | (a) Photograph of a dual frequency metamaterial board, (b) measured and simulated microwave power transmission results for the metamaterials showing two resonance frequency at 2.1 GHz and 2.45 GHz respectively, the inset shows simulated electric field at resonance frequencies in the metamaterial structure – only the resonator with resonance at frequency of incident radiation shows maximum electric field (c) photograph of the patch antenna at 2.1 GHz used for microwave radiation, and (d) simulated and measurement results of the 2.1 GHz patch antenna, inset shows simulated antenna power radiation pattern.

Microwave output power from the power amplifier was increased in steps from 2 W to 50 W. Plasma was ignited (in argon gas at pressure of 40 Torr) at the power level of 30 W in the set of resonators of the same frequency as that of the incoming microwave radiation. The power level was further increased up to 50 W and at this power level plasma starts in the patch antenna itself (at the SMA connector position). This essentially limits the maximum power level of patch antenna that can be transmitted. Power level of 40 W was set to generate the plasma for the photographs reported in this paper. The experiment is repeated with microwave radiation once at 2.1 GHz and another at 2.45 GHz to correspond to the two different resonance frequencies of the metamaterial. Figure 3 shows that microplasma is generated in one set of resonators when excited at 2.1 GHz (Fig. 3a) and in another set of resonators when excited at 2.45 GHz (Fig. 3b). In both cases, there was one resonator that did not produce any plasma. This is attributed to the increase in the gap size of the resonators (0.203 mm and 0.198 mm instead of the expected 0.15 mm) due to fabrication error which resulted in reduced electric field intensity not sufficient for the generation of plasma in these resonators. Total radiated power from the antenna can be estimated from the simulated antenna efficiency. Considering the cable and connector losses of 0.6 dB, the maximum radiated power from antennas at 2.1 GHz is 14 W and at 2.45 GHz is 23 W. Due to higher radiated microwave power at 2.45 GHz than 2.1 GHz, a larger size microplasma is observed in Fig. 3 (b) than in

Fig. 3 (a). The incident power per unit cell can at maximum be 0.78 W (14 W/18) at 2.1 GHz and 1.28 W at 2.45 GHz. The actual power that causes microplasma ignition will be lower since some power radiated from the antenna is not directly incident and is either reflected or scattered by the metamaterial board. Exact determination of the power levels was not currently possible in our experimental setup.
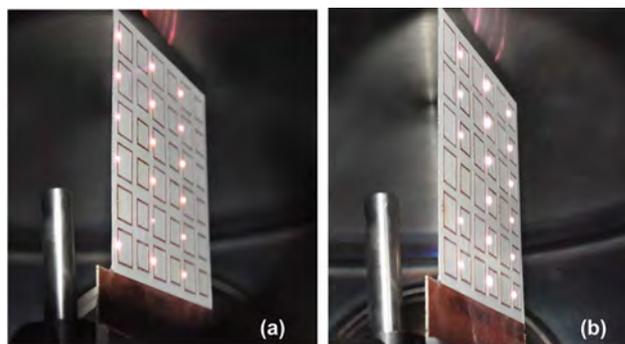

Figure 3 | **Wireless plasma generation in dual frequency metamaterials in argon gas at pressure of 40 Torr.** Plasma is generated in only array of resonators working at (a) 2.1 GHz and (b) 2.45 GHz.
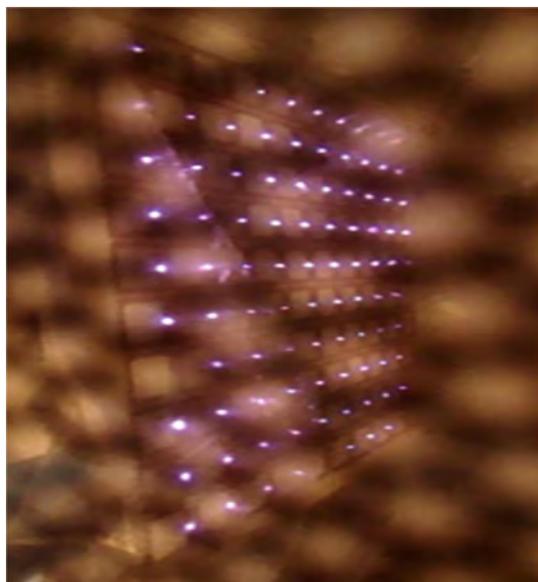
Figure 4 | Metamaterial board of 10 × 10 elements generating plasma at atmospheric pressure and microwave frequency of 2.45 GHz. Plasma is generated in 90 elements out of 100 elements. Photograph is taken through a metal mesh.

For the generation of a larger array of microplasma, a metamaterial board consisting 10 × 10 unit cells with a single resonance frequency of 2.45 GHz is designed (supplementary section Fig. S5). Also, one important parameter of interest for plasma generation, especially for electronic applications, is the carrier concentration in plasma; and it increases with the increase in the gas pressure. Generating plasma at atmospheric pressure (760 Torr) is therefore useful in order to increase the carrier concentration. Plasma generation at atmospheric pressure was investigated in a single frequency metamaterial board consisting 100 unit cells. Paschen's Law describes that higher microwave power is required to initiate plasma at higher gas pressure. A pulsed microwave source with peak power of 500 W (available in conventional commercial microwave oven) is used to generate the plasma at atmospheric pressure at a single frequency of 2.45 GHz. The photograph of the metamaterial with plasma at atmospheric pressure in argon is shown in Fig. 4. Plasma is generated in 90 resonators out of 100 elements (90% yield); fabrication error was responsible for the unit cells that did not ignite. Measurement of carrier density was not possible with the current setup. Morjevi et al. has reported an electron density of 2.4×10^{12} cm^{-3} in microwave argon plasma at atmospheric pressure which was an order of magnitude higher than the plasma at 50 Torr[42]. Recently, in our prior work, Hopwood et al. measured electron density of 3×10^{14} cm^{-3} in atmospheric pressure argon microwave plasma[43].

While one can utilize an array of microplasmas for a variety of applications, we exploit the high nonlinearity of plasmas to realize a non-linear metamaterial. Nonlinear metamaterials are an emerging class of artificial materials with exciting applications in frequency generation[44–46] and parametric amplification[47,48]; they are realized today using varactor loaded split ring resonators which are difficult to scale up due to electrical routing requirements. The electromagnetic properties of the metamaterial medium can be altered by changing the capacitance of the varactor in the gap of each unit cell[45] and in our case by the nonlinearity of the microplasma in the gap of each split ring resonators. These change of nonlinearity with incident field can be exploited for harmonic generation[45].

Of these applications, we show preliminary results of higher order harmonic generation; single sources of plasma have been utilized in the past for harmonics generation[49]. To observe this nonlinear effect,

the emitted spectrum from the metamaterial is recorded where harmonics of the excitation sources can be seen. The measurements show power levels of fundamental frequency (2.45 GHz, −13 dBm), second harmonic (4.9 GHz, −51 dBm), third harmonic (7.35 GHz, −49 dBm) and fourth harmonic (9.8 GHz, −57 dBm) (see supplementary section Fig. S6). The results, while not optimized for this application, clearly indicate that metamaterials can be used as an array to generate high frequency power using higher order harmonic generation. Other applications such as a gain medium using parametric amplification can also be envisioned[44,45].

Discussion

Metamaterials enable a unique application working as a substrate for the remote generation of spatially defined arrays of microplasma. Frequency selective spatial localization of microplasma in a large array can be realized using multiple resonators. Results for a metamaterial with a dual resonator configuration showed that microplasmas are generated spatially in only selected resonators whose resonance frequency is matched to that of incident radiation. Since microwave energy can be fed wirelessly to the metamaterials, the results demonstrate a remote generation of arrays of spatially localized subwavelength microplasmas without the use of any wires. Moreover the electron density in the argon plasma at atmospheric pressure can be much higher than at lower pressure, providing a unique electronic material system with possibly novel functions. Since microplasma could be generated over a large area with a spatially defined pattern, it could be used for many applications such as in the realization of a high-frequency source, where one could exploit the nonlinearity of the plasma for higher order harmonic generation and parametric amplification. This is especially promising in making devices for the terahertz gap in the electromagnetic spectrum.

Methods

1. Veselago, V. G. Electrodynamics of Substances with Simultaneously Negative Values of Sigma and Mu. *Sov. Phys. Usp.-Ussr* **10**, 509, DOI:10.1070/Pu1968v010n04abeh003699 (1968).
2. Pendry, J. B. Negative Refraction Makes a Perfect Lens. *Phys. Rev. Lett.* **85**, 3966 (2000).
3. Pendry, J. B., Schurig, D. & Smith, D. R. Controlling electromagnetic fields. *Science* **312**, 1780–1782, DOI:10.1126/Science.1125907 (2006).
4. Xiao, S. M. *et al.* Loss-free and active optical negative-index metamaterials. *Nature* **466**, 735–U736, DOI: 10.1038/Nature09278 (2010).
5. Smith, D. R., Pendry, J. B. & Wiltshire, M. C. K. Metamaterials and negative refractive index. *Science* **305**, 788–792, DOI: 10.1126/Science.1096796 (2004).
6. Schurig, D. *et al.* Metamaterial electromagnetic cloak at microwave frequencies. *Science* **314**, 977–980, DOI: 10.1126/Science.1133628 (2006).
7. Valentine, J., Li, J. S., Zentgraf, T., Bartal, G. & Zhang, X. An optical cloak made of dielectrics. *Nat. Mater.* **8**, 568–571, doi:Doi 10.1038/Nmat2461 (2009).
8. Landy, N. I., Sajuyigbe, S., Mock, J. J., Smith, D. R. & Padilla, W. J. Perfect metamaterial absorber. *Phys. Rev. Lett.* **100**, 207402, DOI:10.1103/Physrevlett.100.207402 (2008).
9. Singh, P. K., Ameri, S. K., Chao, L., Afsar, M. N. & Sonkusale, S. Broadband Millimeterwave Metamaterial Absorber Based on Embedding of Dual Resonators. *Prog. Electromagn. Res.* **142**, 625–638, DOI: 10.2528/Pier13070209 (2013).
10. Singh, P. K., Korolev, K. A., Afsar, M. N. & Sonkusale, S. Single and dual band 77/95/110 GHz metamaterial absorbers on flexible polyimide substrate. *Appl. Phys. Lett.* **99**, 264101, DOI: 10.1063/1.3672100 (2011).

11. Singh, P. K., Mutzel, C., McNaughton, S. & Sonkusale, S. In-Situ Large Area Fabrication of Metamaterials on Arbitrary Substrates Using Paint Process. *Prog. Electromagn. Res.* **141**, 117–133, DOI: 10.2528/Pier13050313 (2013).

12. Chen, H. T. *et al.* Active terahertz metamaterial devices. *Nature* **444**, 597–600, DOI: 10.1038/Nature05343 (2006).

13. Rout, S., Shrekenhamer, D., Sonkusale, S. & Padilla, W. Embedded HEMT/ Metamaterial Composite Devices for Active Terahertz Modulation. *2010 23rd Annual Meeting IEEE Photon. Soc.* 437–438, DOI: 10.1109/ Photonics.2010.5698947 (2010).

14. Shrekenhamer, D. *et al.* Experimental Realization of a Metamaterial Detector Focal Plane Array. *Phys. Rev. Lett.* **109**, 177401, DOI: 10.1103/ Physrevlett.109.177401 (2012).

15. Strikwerda, A. C. *et al.* Metamaterial Based Terahertz Detector. *2011 CLEO* (2011).

16. Shrekenhamer, D., Watts, C. M., Montoya, J., Krishna, S. & Padilla, W. J. Metamaterial-based imaging for potential security applications. *Photons and Phononic Properties of Engineered Nanostructures III* **8632**, 863221, DOI: 10.1117/ 12.2013145 (2013).

17. Hunt, J. *et al.* Metamaterial Apertures for Computational Imaging. *Science* **339**, 310–313, DOI: 10.1126/Science.1230054 (2013).

18. Pfeiffer, C. & Grbic, A. Metamaterial Huygens' Surfaces: Tailoring Wave Fronts with Reflectionless Sheets. *Phys. Rev. Lett.* **110**, 197401, DOI: 10.1103/ Physrevlett.110.197401 (2013).

19. Sakai, O., Iio, S. & Nakamura, Y. Overdense Microwave Plasma Generation in a Negative-Permeability Space. *Plasma Fusion Res.* **8**, 6 (2013).

20. Nakamura, Y. & Sakai, O. High-density microwave plasma source using negative-permeability metamaterial with tuned wave attenuation. *Jpn. J. Appl. Phys.* **53**, 5 (2014).

21. Becker, K. H., Schoenbach, K. H. & Eden, J. G. Microplasmas and applications. *J. Phys. D-Appl. Phys.* **39**, R55–R70, DOI: 10.1088/0022-3727/39/3/R01 (2006).

22. Ito, T., Izaki, T. & Terashima, K. Application of microscale plasma to material processing. *Thin Solid Films* **386**, 300–304, DOI: 10.1016/S0040-6090(00)01670-9 (2001).

23. Weber, L. F. History of the plasma display panel. *IEEE Trans. on Plasma Sci.* **34**, 268–278, DOI: 10.1109/Tps.2006.872440 (2006).

24. Choi, B. B. *et al.* Nonthermal Plasma-Mediated Cancer Cell Death; Targeted Cancer Treatment. *J Therm. Sci. Technol.* **7**, 399–404, DOI: 10.1299/Jtst.7.399 (2012).

25. Choi, J. H., Lee, H. W., Lee, J. K., Hong, J. W. & Kim, G. C. Low-temperature atmospheric plasma increases the expression of anti-aging genes of skin cells without causing cellular damages. *Arch. Dermatol. Res.* **305**, 133–140, DOI: 10.1007/S00403-012-1259-8 (2013).

26. Fridman, G. *et al.* Floating electrode dielectric barrier discharge plasma in air promoting apoptotic behavior in melanoma skin cancer cell lines. *Plasma Chem. Plasma Process.* **27**, 163–176, DOI: 10.1007/S11090-007-9048-4 (2007).

27. Iza, F. *et al.* Microplasmas: Sources, Particle Kinetics, and Biomedical Applications. *Plasma Process. Polym.* **5**, 322–344, DOI: 10.1002/ppap.200700162 (2008).

28. Kang, S. K. *et al.* Reactive hydroxyl radical-driven oral bacterial inactivation by radio frequency atmospheric plasma. *Appl. Phys. Lett.* **98**, 143702, DOI: 10.1063/ 1.3574639 (2011).

29. Park, G. Y. *et al.* Atmospheric-pressure plasma sources for biomedical applications. *Plasma Sources Sci. Technol.* **21**, 043001, DOI: 10.1088/0963-0252/ 21/4/043001 (2012).

30. Park, J. K. *et al.* Feasibility of nonthermal atmospheric pressure plasma for intracoronal bleaching. *Int. Endod. J.* **44**, 170–175, DOI: 10.1111/J.1365-2591.2010.01828.X (2011).

31. Hensel, K., Machala, Z. & Tardiveau, P. Capillary microplasmas for ozone generation. *Eur. Phys. J.-Appl. Phys.* **47**, 22813, DOI: 10.1051/Epjap/2009077 (2009).

32. Shimizu, K., Masamura, N. & Blajan, M. Water Purification by Using Microplasma Treatment. *11th APCPST and 25th SPSM* **441**, 012005, DOI:10.1088/1742-6596/441/1/012005 (2013).

33. Shimizu, K., Ishii, T. & Blajan, M. Emission Spectroscopy of Pulsed Power Microplasma for Atmospheric Pollution Control. *IEEE Trans. Ind. Appl.* **46**, 1125–1131, DOI: 10.1109/Tia.2010.2044968 (2010).

34. Hoskinson, A. R., Singh, P. K., Sonkusale, S. & Hopwood, J. Low-Voltage Switchable Microplasma Arrays Generated Using Microwave Resonators. *IEEE Electron Device Lett.* **34**, 804–806, DOI: 10.1109/Led.2013.2257659 (2013).

35. Wagner, C. J., Tchertchian, P. A. & Eden, J. G. Coupling electron-hole and electron-ion plasmas: Realization of an npn plasma bipolar junction phototransistor. *Appl. Phys. Lett.* **97**, 134102, DOI: 10.1063/1.3488831 (2010).

36. Cai, M. M., Chowdhury, F. K. & Tabib-Azar, M. Micro-Plasma Field-Effect Transistors. *2012 IEEE Sensors Proc.* 17–20 (2012).

37. Hopwood, J., Iza, F., Coy, S. & Fenner, D. B. A microfabricated atmospheric-pressure microplasma source operating in air. *J. Phys. D-Appl. Phys.* **38**, 1698–1703, DOI:10.1088/0022-3727/38/11/009 (2005).

38. Iza, F. & Hopwood, J. A. Low-power microwave plasma source based on a microstrip split-ring resonator. *IEEE Trans. Plasma Sci.* **31**, 782–787, DOI:10.1109/Tps.2003.815470 (2003).

39. Hoskinson, A. R. & Hopwood, J. A two-dimensional array of microplasmas generated using microwave resonators. *Plasma Sources Sci. Technol.* **21**, 052002, DOI:10.1088/0963-0252/21/5/052002 (2012).

40. Wu, C., Zhang, Z. B., Hoskinson, A. & Hopwood, J. Circular array of stable atmospheric pressure microplasmas. *Eur. Phys. J. D* **60**, 621–625, DOI: 10.1140/ Epjd/E2010-00211-8 (2010).

41. Zhang, Z. B. & Hopwood, J. Linear arrays of stable atmospheric pressure microplasmas. *Appl. Phys. Lett.* **95**, 161502, DOI: 10.1063/1.3251793 (2009).

42. Moravej, M. *et al.* Physics of high-pressure helium and argon radio-frequency plasmas. *J. Appl. Phys.* **96**, 7011–7017, DOI:10.1063/1.1815047 (2004).

43. Hoskinson, A. R. & Hopwood, J. Spatially resolved spectroscopy and electrical characterization of microplasmas and switchable microplasma arrays. *Plasma Sources Sci. Technol.* **23**, 015024, DOI:10.1088/0963-0252/23/1/015024 (2014).

44. Klein, M. W., Enkrich, C., Wegener, M. & Linden, S. Second-Harmonic Generation from Magnetic Metamaterials. *Science* **313**, 502–504, DOI: 10.1126/ science.1129198 (2006).

45. Shadrivov, I. V., Kozyrev, A. B., van der Weide, D. W. & Kivshar, Y. S. Tunable transmission and harmonic generation in nonlinear metamaterials. *Appl. Phys. Lett.* **93**, 161903, DOI:http://dx.doi.org/10.1063/1.2999634 (2008).

46. Huang, D., Rose, A., Poutrina, E., Larouche, S. P. & Smith, D. R. Wave mixing in nonlinear magnetic metacrystal. *Appl. Phys. Lett.* **98**, 204102, DOI:http://dx.doi.org/10.1063/1.3592574 (2011).

47. Popov, A. K. & Shalaev, V. M. Negative-index metamaterials: second-harmonic generation, Manley, ÀìRowe relations and parametric amplification. *Appl. Phys. B* **84**, 131–137, DOI:10.1007/s00340-006-2167-4 (2006).

48. Poutrina, E., Larouche, S. P. & Smith, D. R. Parametric oscillator based on a single-layer resonant metamaterial. *Opt. Commun.* **283**, 1640–1646, DOI:http://dx.doi.org/10.1016/j.optcom.2009.11.037 (2010).

49. Chiyoda, K. Theory of Harmonic Generation in a Microwave Gaseous Plasma under an External Magnetic Field. *J. Phys. Soc. Jpn.* **22**, 910–&, DOI: 10.1143/ Jpsj.22.910 (1967).

Acknowledgments

Author contributions

P.K.S. and S.S. contributed to development of the concept, design of experiments and writing of the manuscript. P.K.S. conducted the actual simulations, fabrication and measurements. J.H. contributed to the discussion on plasma science and provision of the facility for measurements.

Additional information

Supplementary information accompanies this paper at http://www.nature.com/ scientificreports

Competing financial interests: The authors declare no competing financial interests.

How to cite this article: Singh, P.K., Hopwood, J. & Sonkusale, S. Metamaterials for Remote Generation of Spatially Controllable Two Dimensional Array of Microplasma. *Sci. Rep.* **4**, 5964; DOI:10.1038/srep05964 (2014).